Received: 10 May 2023 | Revised: 17 April 2024 | Accepted: 8 May 2024

DOI: 10.1111/all.16206

Allergy EUROPEAN JOURNAL OF ALLERGY AND CLINICAL IMMUNOLOGY EAACI WILEY

ORIGINAL ARTICLE

Basic and Translational Allergy Immunology

Helminth induced monocytosis conveys protection from respiratory syncytial virus infection in mice

Matthew O. Burgess[1] | Piotr Janas[1] | Karla Berry[1] | Hannah Mayr[1,2] | Matthias Mack[3] | Stephen J. Jenkins[1] | Calum C. Bain[1] | Henry J. McSorley[4] | Jurgen Schwarze[1,5]

[1]Centre for Inflammation Research, Institute for Regeneration and Repair, University of Edinburgh, Edinburgh, UK

[2]Institute of Medical Genetics, Medical University of Vienna, Vienna, Austria

[3]Department of Nephrology, University Hospital Regensburg, Regensburg, Germany

[4]Cell Signalling and Immunology, School of Life Sciences, University of Dundee, Dundee, UK

[5]Child Life and Health, Centre for Inflammation Research, Institute for Regeneration and Repair, University of Edinburgh, Edinburgh, UK

Correspondence
Jurgen Schwarze, Centre for Inflammation Research, Institute for Regeneration and Repair, The University of Edinburgh, Edinburgh BioQuarter, 4-5 Little France Drive, Edinburgh EH16 4UU, UK.
Email: jurgen.schwarze@ed.ac.uk

Abstract

Background: Respiratory syncytial virus (RSV) infection in infants is a major cause of viral bronchiolitis and hospitalisation. We have previously shown in a murine model that ongoing infection with the gut helminth *Heligmosomoides polygyrus* protects against RSV infection through type I interferon (IFN-I) dependent reduction of viral load. Yet, the cellular basis for this protection has remained elusive. Given that recruitment of mononuclear phagocytes to the lung is critical for early RSV infection control, we assessed their role in this coinfection model.

Methods: Mice were infected by oral gavage with *H. polygyrus*. Myeloid immune cell populations were assessed by flow cytometry in lung, blood and bone marrow throughout infection and after secondary infection with RSV. Monocyte numbers were depleted by anti-CCR2 antibody or increased by intravenous transfer of enriched monocytes.

Results: *H. polygyrus* infection induces bone marrow monopoiesis, increasing circulatory monocytes and lung mononuclear phagocytes in a IFN-I signalling dependent manner. This expansion causes enhanced lung mononuclear phagocyte counts early in RSV infection that may contribute to the reduction of RSV load. Depletion or supplementation of circulatory monocytes prior to RSV infection confirms that these are both necessary and sufficient for helminth induced antiviral protection.

Conclusions: *H. polygyrus* infection induces systemic monocytosis contributing to elevated mononuclear phagocyte numbers in the lung. These cells are central to an antiviral effect that reduces the peak viral load in RSV infection. Treatments to promote or modulate these cells may provide novel paths to control RSV infection in high risk individuals.

KEYWORDS
helminth, innate immunity, mononuclear phagocyte, RSV, virus

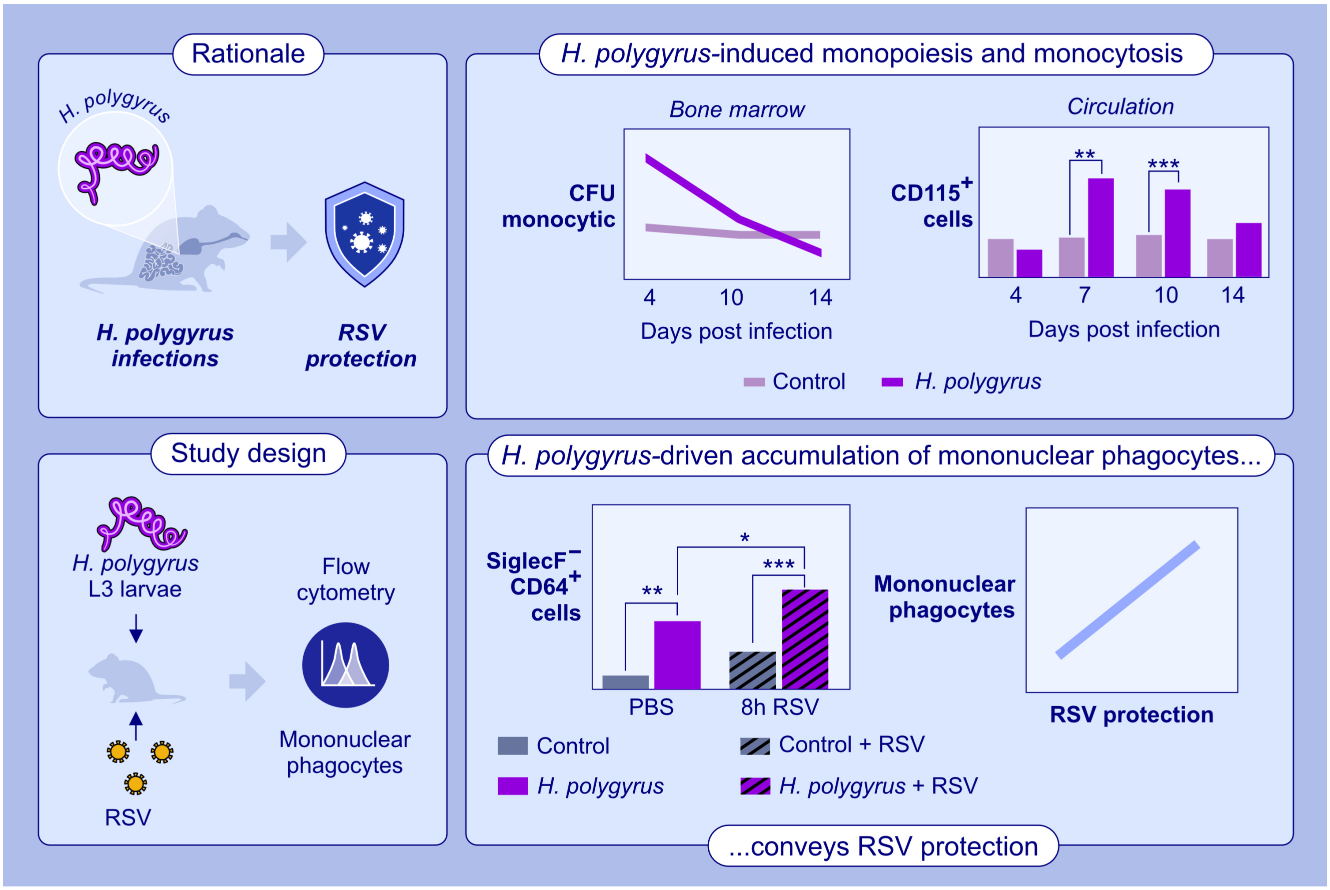

GRAPHICAL ABSTRACT

Ongoing *H. polygyrus* infection in mice induces bone marrow monopoiesis, circulatory monocytosis and increases lung mononuclear phagocytes. *H. polygyrus* infection increases the accumulation of lung mononuclear phagocytes in the early immune response to RSV. Lung mononuclear phagocyte numbers are proportional to the capacity to control RSV. Abbreviations: CFU, colony forming units; *H. polygyrus*, *Heligmosomoides polygyrus*, RSV, respiratory syncytial virus.

1 | INTRODUCTION

Respiratory syncytial virus (RSV) induced viral bronchiolitis is a major cause of infant hospitalisation worldwide.[1] Adult infection is frequently associated with mild respiratory illness but can also cause significant morbidity and mortality in the elderly and immunocompromised individuals.[2,3] For children, there is as yet no active vaccination against RSV infection and no specific therapy although many promising candidates are currently in clinical trials. Treatment is limited to supportive measures and prophylaxis for high risk infants with the anti-RSV F-protein antibody palivizumab, a high cost option with limited effectiveness.[4,5] The impact of nirsevimab, a novel anti-RSV F-protein antibody intended to be given to all infants, is yet to be established.

Novel approaches to managing RSV, and greater understanding of the immune response to infection, are still required. We have previously reported that an ongoing infection with the murine enteric helminth *Heligmosomoides polygyrus* is able to improve RSV infection outcomes by suppressing the peak viral load early in infection.[6] This work found that the adaptive immune response to *H. polygyrus* infection, the type 2 immune response, characteristic of helminthic infection and typified by robust IL-33, IL-4 and IL-13 signalling,[7] as well as the anti-microbial peptide LL-37 are not required for the *H. polygyrus* induced anti-viral immunity in the lung. Rather, type I interferon (IFN-I) signalling, induction of interferon beta (IFNβ) and interferon stimulated genes (ISGs), including *Rsad2* (encoding viperin) and *Oas1a* (2′-5′-oligoadenylate synthetase 1) are central to the *H. polygyrus* induced protective effect against RSV infection. Many ISGs have antiviral functions and both viperin and OAS can limit RSV infection.[8,9] Almost all cells of the lung have the capacity to both produce one or more of the family of IFN-Is and to respond to IFN-I signalling through the dedicated receptor IFNalpha receptor (Infar).[10–12] This broad potential space for IFN-I signalling led us to question which cells may be contributing to *H. polygyrus* induced anti-viral effects. Mononuclear phagocytes, including monocytes and macrophages, are known responders to IFN-Is and have been linked to early control of RSV infection.[13,14] IFN-Is can regulate monocyte recruitment during inflammation, skew hematopoietic output and through interferon regulatory factors promote differentiation to, and polarisation of, macrophages.[15–18] Monocytes can also be potent producers of IFN-Is, especially IFNβ, in response to stimuli including RSV.[19] We therefore hypothesised that lung mononuclear phagocytes following *H. polygyrus* infection mediate the helminth induced protective effect against RSV infection.

2 | MATERIALS AND METHODS

2.1 | Animals

BALB/c mice were purchased from Charles River (Margate, Kent, UK). C57BL/6 and *Ifnar1*$^{-/-}$ (C57BL/6 background)[20] mice were bred in-house at the University of Edinburgh. Eight–12 week old mice were infected by oral gavage with 200 stage 3 *H. polygyrus* larvae. Some animals were administered 20 μg of anti-CCR2 antibody (MC-21, gift M. Mack) or IgG2b isotype control (402202; Biolegend; London, UK) by intra-peritoneal injection 7 and 9 days later. Other animals were given 2×10^6 enriched bone marrow monocytes by intravenous injection. Some animals were infected with RSV (10^5 plaque forming units) intranasally 10 days after *H. polygyrus* infection. After monocyte transfer RSV was administered 30 min later. Some animals were administered 0.7 μg Brilliant Violet 785 CD45 (30-F11; Biolegend; London, UK) immediately prior to cull to label circulatory cells. All procedures were approved by local ethical review committee and the UK Home Office.

2.2 | Parasites and viral stocks

The parasite life cycle was maintained as previously described.[21] Plaque-purified human RSV (Strain A2; ATCC, VA, USA) was grown in HEp-2 cells as previously described.[22]

2.3 | RSV immunoplaque assay

RSV titres were assessed by immunoplaque assay. Lung homogenates were titrated onto HEp-2 cell monolayers in 96-well plates. Twenty-four hours later monolayers were fixed and permeabilised with 2% H_2O_2 in methanol then bound with biotin-conjugate goat anti-RSV antibody (BioRad; Watford, Hertfordshire, UK). Plaques were visualised with extravidin peroxidase and AEC red (SigmaAldrich; Glasgow, Scotland, UK) and infection units observed by light microscopy.

2.4 | L-gene real time PCR

Lungs were homogenized in 1 mL of TRIzol (ThermoFisher Scientific; Waltham, MA, USA). cDNA was made from the 2 μg extracted RNA using HC cDNA RT kit (ThermoFisher Scientific; Waltham, MA, USA) according to manufacturer's instructions. Custom primers and probe for RSV L gene were used as previously described.[6]

2.5 | Colony forming assays

Bone marrow colony forming assays were performed with MethoCult GF M3434 (StemCell Technologies; Cambridge, Cambridgeshire, UK) per manufacturer's instructions. Bone marrow from hind limb tibia and femur flushes was washed, 70 μm filtered and then resuspended in MethoCult GF M3434 at 1×10^4 cells per 35 mm culture dish in duplicate. Plates were incubated at 37°C 5% CO_2 in humidified chambers. After 10–12 days colonies were assigned to different lineage by morphological examination under light microscopy and counted.

2.6 | Flow cytometry

Following digestion with Liberase (385 μg/mL PBS; SigmaAldrich; Glasgow, Scotland, UK) and DNaseI (0.5 mg/mL; SigmaAldrich; Glasgow, Scotland, UK) and red blood cell lysis (Hybrimax buffer; SigmaAldrich; Glasgow, Scotland, UK) 2×10^6 lung cells per panel were stained with LIVE/DEAD fixable near-IR dead cell kit (ThermoFisher Scientific; Waltham, MA, USA). The following anti-mouse antibodies were used for immune cell characterisation; Brilliant Violet 510 CD11c (N418; Biolegend; London, UK), Brilliant Violet 570 CD11b (M1/70; Biolegend; London, UK), Brilliant Violet 605 CD45 (30-F11; Biolegend; London, UK), AlexaFluor 647 CD64 (X54-5/7.1; Biolegend; London, UK), AlexaFluor 700 Ly6C (HK1.4; Biolegend; London, UK), PE/Cyanine7 CD301 (LOM-14; Biolegend; London, UK), phycoerythrin Siglec-F (E50-2440; BD Biosciences; Wokingham, Berkshire, UK), eFluor 450 Ly6G (1A8; ThermoFisher Scientific; Waltham, MA, USA). Fc-receptor binding was blocked using anti-mouse CD16/CD32 antibody (2.4G2) (BD Biosciences; Wokingham, Berkshire, UK) (Figure S1A).

Red blood cell were lysed (RBC lysis buffer; Biolegend; London, UK) and 50 μL per panel was stained with dead cell kit as above and the following antibodies used; Lineage dump (Brilliant Violet 421 Siglec F (E50-2440; BD Biosciences), Pacific Blue CD3 (17A2; Biolegend; London, UK), CD19 (6D5; Biolegend; London, UK) and CD49b (PK136; Biolegend; London, UK)), Brilliant Violet 510 Ly6G (1A8; Biolegend; London, UK), Brilliant Violet 605 CD45 (30-F11; Biolegend; London, UK), Brilliant Violet 650 CD11b (M1/70; Biolegend; London, UK), phycoerythrin Treml4 (16E5; Biolegend; London, UK), allophycocyanin CD115 (AFS98; Biolegend; London, UK), AlexaFluor 700 Ly6C (HK1.4; Biolegend; London, UK). Fc-receptor binding was blocked as above (Figure S1B).

2×10^6 bone marrow cells were stained with dead cell kit as above, lineage dump (as above plus Pacific Blue Ly6G (1A8; Biolegend; London, UK), TER-119 (TER-119; Biolegend; London, UK), CD11c (N418; Biolegend; London, UK)), BV711 CD16/CD32 (93; Biolegend; London, UK), PE-Cy7 CD117 (2B8; Biolegend; London, UK), allophycocyanin CD115 (AFS98; Biolegend; London, UK) and AlexaFluor 700 Ly6C (HK1.4; Biolegend; London, UK). Fc-receptor binding was blocked using purified mouse serum (M5905; SigmaAldrich; Glasgow, Scotland, UK) (Figure S1C).

Flow cytometry samples were analysed with an Aurora cytometer (Cytek; Amsterdam, The Netherlands) with SpectroFlo® v3 (Cytek; Amsterdam, The Netherlands) and analysis performed with FCS Express 7 (De Novo Software; Pasadena, CA, USA). Ly6C$^+$ SiglecF$^-$ CD64$^+$ mononuclear phagocytes were isolated with a BD FACS Aria Fusion (5 laser, 100 μm nozzle; BD Biosciences; Wokingham, Berkshire, UK).

2.7 | Monocyte isolation

To enrich bone marrow monocytes for cell transfer experiments mouse monocyte isolation Kit (130-100-629; Miltenyi Biotec; Bisley, Surrey, UK) was used.

2.8 | RNA isolation and NanoString

Ly6C+ SiglecF− CD64+ mononuclear phagocytes were FACS-sorted, and RNA was isolated using the RNAqueous®-Micro Kit (AM1931; ThermoFisher Scientific; Waltham, MA, USA). A total of 12 samples were profiled using the nCounter Analysis System by HTPU staff according to NanoString nCounter guidelines. NanoString Mouse Immunology Panel (XT-CSO-MIM1-12; NanoString; Seattle, WA, USA) and nCounter Masterkit (NAA-AKIT-012; NanoString; Seattle, WA, USA). In brief, hybridization tubes were prepared by combining 6.7 μL of 15 ng/μL RNA (100 ng total RNA) with 8 μL of hybridization buffer containing reporter CodeSet and 2 μL Capture Probeset. Following an 18-h hybridization reaction, the samples were processed using the High Sensitivity protocol. Subsequently, the samples were purified, immobilized and cartridges were read using 555 fields of view.

The NanoString RCC files underwent processing, quality control (QC) and analysed using RStudio R4.3.1 'NanoTube' package (release 3.18).[23] All samples passed positive QC, with scaling factors falling within the recommended range of 0.3–3, and R-squared values greater than 0.95. Next, negative QC was performed, and background thresholds were determined for each sample, followed by calculating housekeeping normalization scale factors. The housekeeping scale factors for each sample fell within the recommended range of 0.1–10. The samples were normalized using RUVg method from the 'RUVSeq' package (release 1.36.0)[24] with number of unwanted factors set to '1', and bgPVal set to '0.05'. The remaining RUVg normalization parameters were set to default. The normalized data generated using RUVg was used to create heatmaps, or for further differential analysis using 'limma' package (release 3.18).[25] Differential analysis results were used to generate volcano plots of −log10(q) and log2FC values using 'ggplot2' package (release 3.5) and 'ggrepel' package (release 0.9.5).

2.9 | Statistical analysis

All data were analysed using Prism 9 software (GraphPad Software; Boston, MA, USA). Data from two groups were analysed by unpaired *t*-test, while data from more than two groups were analysed by one-way ANOVA with Tukey's multiple comparisons test with a single pooled variance. Unless otherwise stated, differences are statistically non-significant. *$p < .05$, **$p < .01$, ***$p < .001$, ****$p < .0001$.

3 | RESULTS

3.1 | H. polygyrus infection induces blood monocytosis and increases lung mononuclear phagocytes

The early response to RSV infection in mice drives the recruitment of monocytes to the lung causing an accumulation of mononuclear phagocytes.[13] In the initial hours of infection these cells are predominantly Ly6C^{hi}, later downregulating Ly6C and becoming predominantly CD11c^{+}. Flow cytometric analysis was used to assess if these populations were also affected by *H. polygyrus* infection. Female BALB/c mice were infected with *H. polygyrus* and lungs assessed for innate immune cell composition through the later stages of infection. Cells of the monocyte–macrophage lineage were identified by their expression of the high affinity Fc receptor, CD64 (also known as FcγR1), and subdivided on the basis of SiglecF expression. SiglecF expressing CD64^{+} cells represent alveolar macrophages, whereas the SiglecF^{-} compartment will contain interstitial macrophages and some monocytes and their progeny, hereby referred to as mononuclear phagocytes. Compared with sham infection controls there was an increase in the numbers of mononuclear phagocytes (CD45^{+}, Ly6G^{-}, SiglecF^{-}, CD11b^{+}, CD64^{+}, Figure 1A) in the lungs of *H. polygyrus* infected mice from 10 days post infection, subsiding yet still elevated at 14 days (Figure 1B). In comparison, the resident alveolar macrophage compartment (CD45^{+}, Ly6G^{-}, SiglecF^{+}, CD11b^{-}, CD64^{+}, Figure 1A) remained unchanged (Figure 1C). The expansion was predominantly due to Ly6C^{+} mononuclear phagocytes with a variable increase in CD11c^{+} only at day 10 (Figure 1D–F).

A large proportion of the recruited macrophages seen in response to lung inflammatory stimuli are derived from circulating monocytes.[26,27] It is therefore likely that the vascular monocyte reservoir would reflect the observed influx of mononuclear phagocytes to the lung. Peripheral blood was sampled from mice throughout *H. polygyrus* infection to assess circulatory monocyte counts by flow cytometry (CD45^{+}, Lin^{-}, CD11b^{+}, Ly6G^{-}, CD115^{+}, Figure 2A). Elevated total monocyte numbers were observed from seven to 10 days post infection (Figure 2B) and their numbers returned to baseline by 14 days post infection. Circulatory monocytes in the mouse can be distinguished into three phenotypic subtypes; classical, intermediate and non-classical monocytes.[28,29] Using the markers Ly6C and Treml4 to separate these three populations (Figure 2A), the *H. polygyrus* induced expansion of monocytes was found to be predominantly in Ly6C^{+}Treml4^{-} classical monocytes (Figure 2C).

In wild mice, *H. polygyrus* is a chronic infection, similar to many human hookworm infections without pharmaceutical intervention.[30,31] To test if protection or monocytosis persist at longer time courses of infection, female BALB/c mice were infected with *H. polygyrus* and the infection left to 35 days post infection (dpi). Long term infected mice were then intranasally infected with RSV and peak viral titre assessed 4 days later (day 39 post *H. polygyrus* infection). Long term *H. polygyrus* infection was not protective against RSV infection (Figure S2A). Blood and lung were collected from mice 35 dpi with

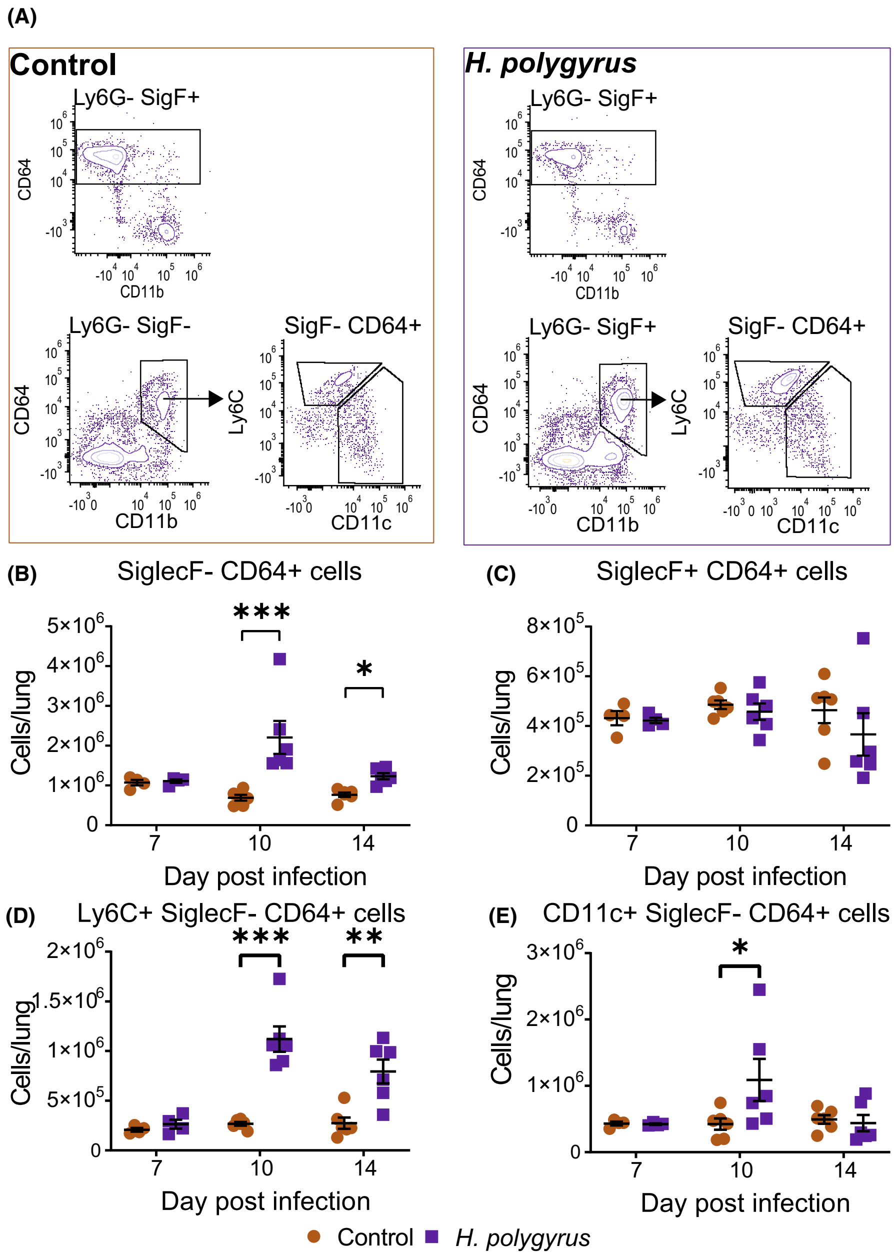

FIGURE 1 *H. polygyrus* infection induces an expansion of lung mononuclear phagocytes. Female BALB/c mice were administered an equal volume of either sterile dH_2O as infection control or 200 *H. polygyrus* L3 larvae by oral gavage. Seven, 10 and 14 days post infection lungs were harvested for flow cytometry analysis. (A) Representative gating strategy for the identification of alveolar macrophages ($CD45^+$, $Ly6G^-$, $SigF^+$, $CD64^+$) and mononuclear phagocytes ($CD45^+$, $Ly6G^-$, $SigF^-$, $CD11b^+$, $CD64^+$) and mononuclear phagocyte subtyping (Ly6C CD11c). (B, C) Absolute numbers of (B) mononuclear phagocytes and (C) alveolar macrophages at the indicated time points post *H. polygyrus* infection. (D-E) Absolute numbers of (D) $Ly6C^+CD11c^-$ and (E) $Ly6C^-CD11c^+$ mononuclear phagocytes at the indicated time points post *H. polygyrus* infection. Symbols represent individual mice with $n=6$ per group pooled from two independent experiments. Statistical significance of difference determined with unpaired two-tailed t-test. *$p<.05$, **$p<.001$, ***$p<.001$.

H. polygyrus and monocyte and mononuclear phagocyte numbers assessed. No change in cell counts was observed for blood monocytes, lung mononuclear phagocytes or their subtypes (Figure S2B–F).

We previously reported that irradiated *H. polygyrus* larvae still confer an anti-RSV effect.[6] Irradiated L3 larvae are still infection competent but fail to moult and mature following invasion of the duodenal wall.[32] Flow cytometry was repeated with female BALB/c mice infected with larvae exposed to 300 Gy immediately prior to infection to test if this was also sufficient to induce monocytosis. An attenuated, and briefer induction of blood monocytes was observed with irradiated larvae, elevating by seven dpi but no longer significantly elevated by 10 dpi (Figure S3A). Nevertheless, this was still sufficient to drive a comparable increase in lung mononuclear phagocytes 10 dpi between irradiated and non-irradiated *H. polygyrus* larvae (Figure S3B). Together these data suggest a correlation between monocytosis and the anti-RSV effects of the early stages of *H. polygyrus* infection.

3.2 | H. polygyrus infection induces bone marrow monopoiesis

Under normal physiological conditions, murine classical monocytes have a half-life of just over 1 day in the circulation, with constant replenishment from the bone marrow.[33,34] To understand if the monocytosis in blood during *H. polygyrus* infection reflected changes at the level of bone marrow haematopoiesis, we used colony forming assays to assess the progenitor lineage potential during *H. polygyrus* infection. Four days post infection there was an increase in the number of monocyte-committed progenitors (Colony Forming

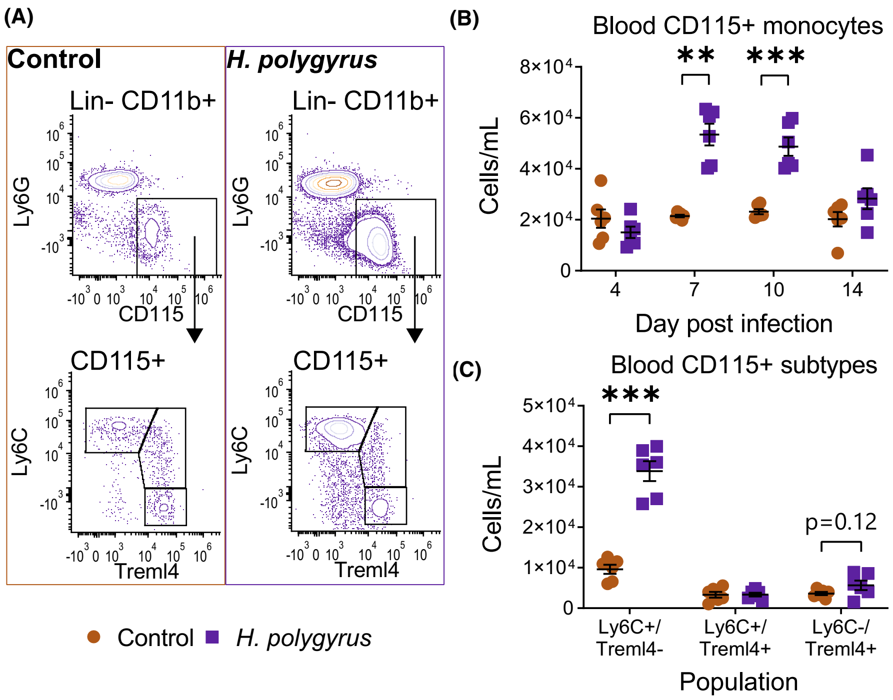

FIGURE 2 *H. polygyrus* infection induces circulatory monocytosis. Female BALB/c mice were administered an equal volume of either sterile dH_2O as infection control or 200 *H. polygyrus* L3 larvae by oral gavage. Seven, 10 and 14 days post infection (dpi) blood samples were collected for flow cytometry analysis. (A) Representative gating strategy for the identification of monocytes ($CD45^+$, $Lineage^-$, $CD11b^+$, $Ly6G^-$, $CD115^+$) and the monocytic subsets—classical ($Ly6C^+$, $Treml4^-$) intermediate ($Ly6C^+$, $Treml4^+$), and non-classical ($Ly6C^-$, $Treml4^+$). (B) Monocyte numbers per mL blood at indicated time points post *H. polygyrus* infection. (C) Numbers of blood monocyte subtypes 10 dpi with *H. polygyrus*. Symbols represent individual mice with $n=6$ per group pooled from two independent experiments. Statistical significance of difference determined with unpaired two-tailed t-test. $^{**}p<.01$, $^{***}p<.001$.

Unit—Monocytic; CFU-M) compared to uninfected controls, no other myeloid progenitor tested was altered (Figure 3A). Although this elevation was short lived and lost by 10 dpi (Figure 3B), enumeration of classical monocytes (Lin^-, $CD16/CD32^+$, $CD117^-$, $CD115^+$, $Ly6C^+$, Figure 3C) in the bone marrow confirmed that their numbers increase in the context of *H. polygyrus* infection (Figure 3D). $Ly6C^-$ non-classical monocytes are unchanged throughout *H. polygyrus* infection, possibly due to their differentiation in vascular niches (Figure 3E).[33–35]

3.3 | H. polygyrus infection induced increases in blood monocytes and lung mononuclear phagocytes are IFN-I signalling dependent

IFN-I signalling through Infar is essential to the *H. polygyrus* induced anti-viral effect.[6] To test if the expansion in mononuclear phagocytes was dependent on this signalling axis, cell counts were assessed 10 dpi with *H. polygyrus* in *Ifnar1*$^{-/-}$ mice, which are maintained on a C57BL/6 background. Importantly, the *H. polygyrus* induced expansion of lung mononuclear phagocytes (Figure 4A), across both $Ly6C^+$ (Figure 4B) and $CD11c^+$ (Figure 4C) mononuclear phagocyte subtypes, and of circulatory monocytes (Figure 4D) were evident in control C57BL/6 mice but was lost in the absence of IFN-I signalling. Classical monocytes ($Ly6C^+$, $Treml4^-$) are the expanded circulatory population in C57BL/6 mice and lost in *Ifnar1−/−* mice (Figure 4E). In contrast, Infar-deficient mice still had increases in committed monocyte progenitors in the bone marrow after *H. polygyrus*, albeit to a lower level than in wild type controls (Figure 4F). $Ly6C^+$ monocyte numbers in the bone marrow were also increased after *H. polygyrus* in *Ifnar1−/−* mice (Figure 4G). $Ly6C^-$ bone marrow monocytes were unchanged (Figure 4H). Alveolar macrophages and neutrophils were unchanged by *H. polygyrus* infection of *Infar1−/−* mice, whilst eosinophils were increased (Figure S4).

3.4 | H. polygyrus monocytosis results in higher numbers of lung mononuclear phagocytes early after RSV infection

RSV induced monocyte influx and subsequent accumulation of lung mononuclear phagocytes is crucial for the production of cytokines associated with the antiviral response.[13] To ascertain if this early influx was altered following *H. polygyrus* infection, we used flow cytometry to assess the monocyte-mononuclear phagocyte compartment 8h post RSV infection. RSV infection alone trended towards an increased number of mononuclear phagocytes in the lung ($p=.13$, Figure 5A), similar to observations of others in C57BL/6 mice,[13] but after prior infection with *H. polygyrus* mononuclear phagocyte counts significantly increased compared to both *H. polygyrus* or RSV infection alone (Figure 5A). This expansion beyond RSV infection alone was seen in

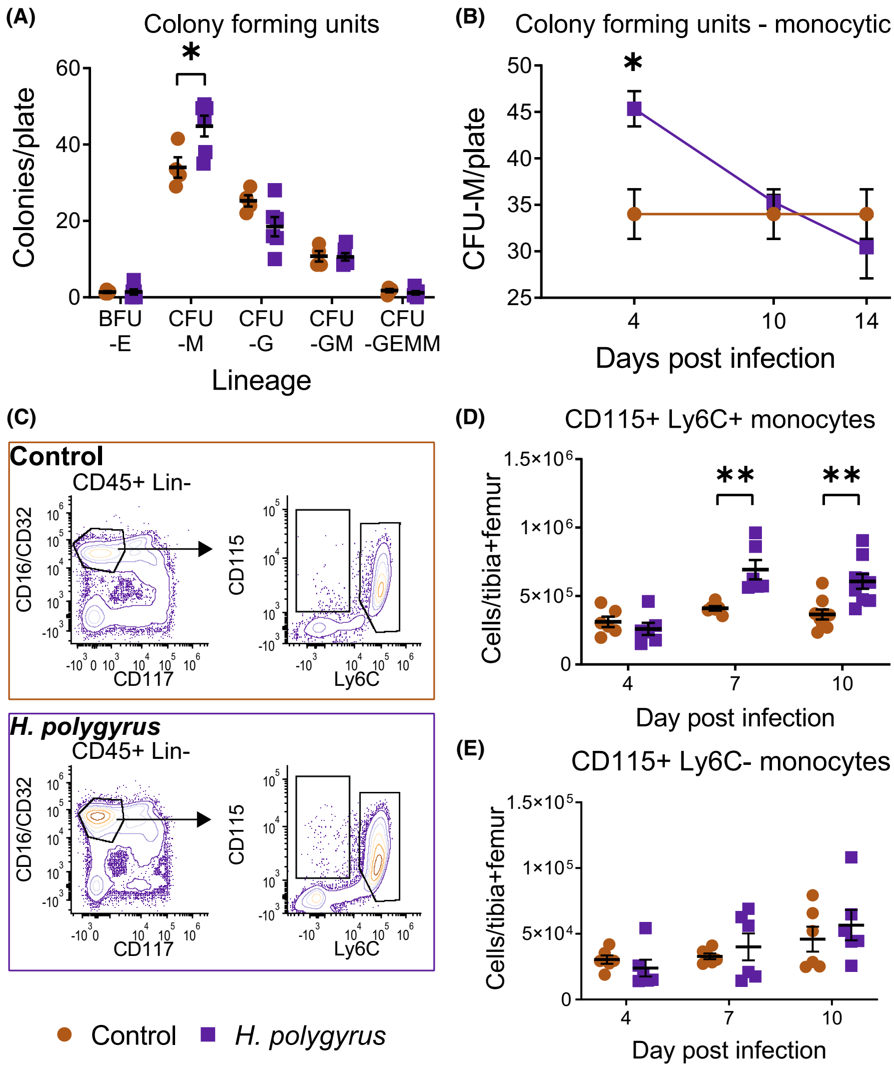

FIGURE 3 *H. polygyrus* infection induces bone marrow monopoiesis. Female BALB/c mice were administered an equal volume of either sterile dH_2O as infection control or 200 *H. polygyrus* L3 larvae by oral gavage. Four, 7, 10 and 14 days post infection (dpi) bone marrow flushes from tibias and femurs were collected for either colony forming assays (CFAs) or flow cytometry analysis. (A) CFAs were performed on hind limb bone marrow 4 dpi, assessing monocytic colony forming units—monocytic (CFU-M), blast forming unit—erythroid (BFU-E), colony forming unit granulocytic (CFU-G), granulocytic/monocytic (CFU-GM), granulocytic/erythroid/monocytic mixed (GEMM). (B) CFU-M counts were also assessed at 10 and 14 dpi. (C) Representative gating strategy for the identification of bone marrow monocytes (lineage$^-$, CD16/CD32$^+$, CD117$^-$, CD115$^+$. Ly6C$^+$ or Ly6C$^-$). (D) Numbers of bone marrow Ly6C$^+$ and (E) Ly6C$^-$ monocytes were assessed throughout *H. polygyrus* infection. Symbols represent individual mice $n=4$ for control and $n=6$ for *H. polygyrus* groups pooled from two independent CFU experiments. Flow cytometry experiments day 4 and 7 $n=6$ per group, day 10 $n=9$ per group. Statistical significance of difference determined with unpaired two-tailed *t*-test. $^*p<.05$, $^{**}p<.01$.

both Ly6C$^+$ and CD11c$^+$ mononuclear phagocytes, but only Ly6C$^+$ mononuclear phagocyte numbers were further elevated beyond *H. polygyrus* infection alone (Figure 5B,C). Four days after RSV infection, numbers of Ly6C$^+$ macrophages remained higher in mice with prior *H. polygyrus* infection (Figure 5D), while the increase in numbers of CD11c$^+$ macrophages did not persist (Figure 5E). Alveolar macrophage numbers were unaffected by prior *H. polygyrus* infection at both 8 and 96 h post RSV infection (Figure S5A,B). These findings demonstrate that *H. polygyrus* infection leads to numbers of lung mononuclear phagocytes that exceed those found early after RSV infection alone, raising the possibility that high numbers of these cells confer an early protective effect against RSV infection.

Flow cytometry analysis of the blood and lung in *H. polygyrus* infection saw different timelines of expansion, suggestive of differential localisation (Figures 1 and 2). Intravenous labelling of circulatory haematopoietic cells using a fluorescently tagged anti-CD45 antibody revealed that the Ly6C$^+$ (Figure 5G) lung mononuclear phagocytes remain closely associated with the vasculature during *H. polygyrus* infection. The proportion of CD45 labelled CD11c$^+$ mononuclear phagocytes increased following *H. polygyrus* infection, potentially demonstrating additional recruitment to the lung vasculature (Figure 5I). Both mononuclear phagocyte populations reduced their intravenous CD45 labelling 24 h post infection with RSV, suggesting this reservoir of lung associated cells migrates into the tissue following viral infection.

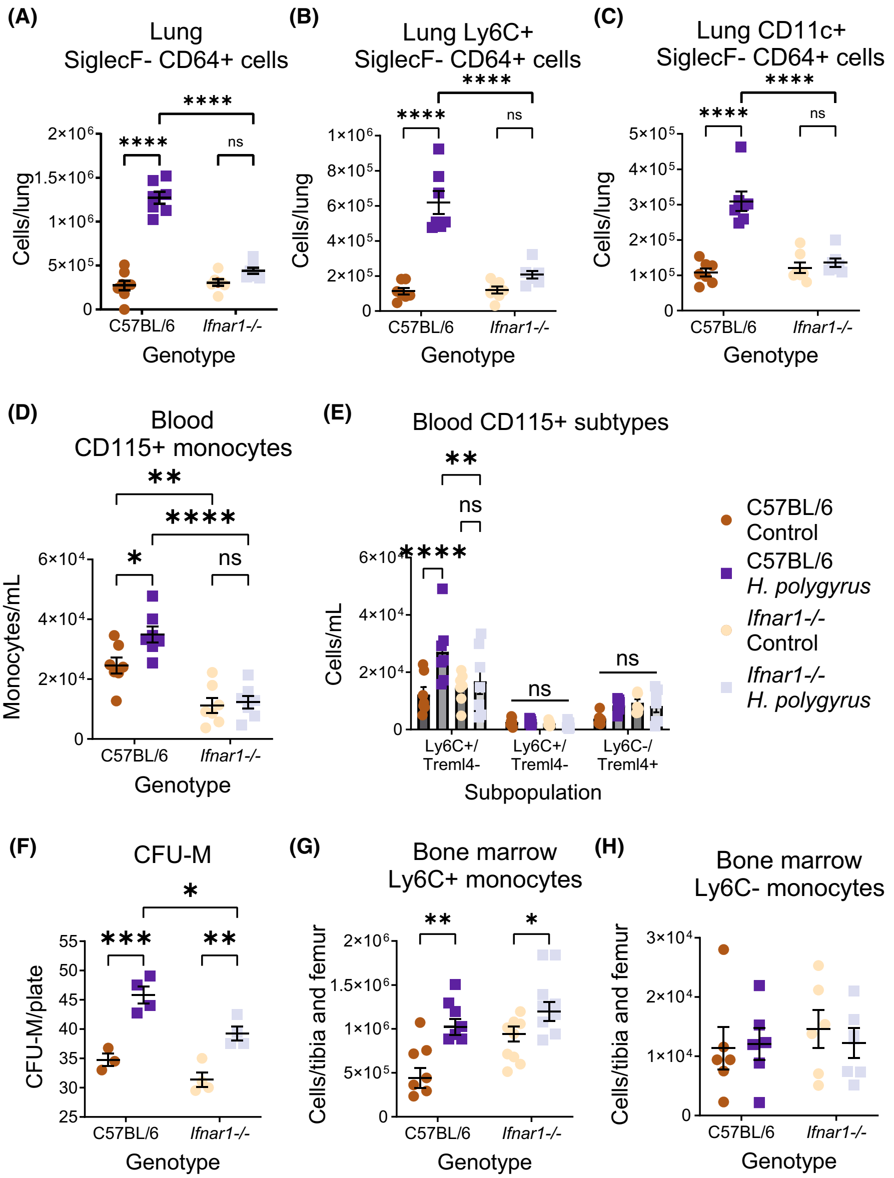

FIGURE 4 Infar signalling is essential for *H. polygyrus* induced blood monocyte and lung mononuclear phagocyte expansion but not bone marrow monopoiesis. Female C57BL/6 or *Ifnar1−/−* mice were administered 200 *H. polygyrus* L3 larvae by oral gavage or an equal volume of sterile dH_2O as infection control. Ten days post infection (dpi) lungs, blood and bone marrow were harvested for flow cytometry analysis and colony forming assays (CFAs) as per Figures 1–3. Comparing C56BL/6 to *Ifnar1−/−* mice (A) lung mononuclear phagocytes (MNPs), (B) $Ly6C^+$ MNPs, (C) $CD11c^+$ MNPs, and blood (D) $CD115^+$ monocytes and (E) $CD115^+$ blood monocyte subtypes were enumerated. (F) Bone marrow CFAs were assessed from hind limb bone marrow with colony forming units—monocytic (CFU-M) presented (other CFA outputs non-significant). (G) Bone marrow $Ly6C^+$ monocytes and (H) $Ly6C^-$ monocytes per tibia and femur were counted. Symbols represent individual mice with $n = 7$ per group pooled from two independent experiments for (A-E, G, H). One experiment of $n = 4$ for CFAs (F). Statistical significance of difference determined with one way ANOVA $^*p < .05$, $^{**}p < .01$, $^{***}p < .001$, $^{****}p < .0001$, ns, not significant.

3.5 | Expanded circulatory monocytes are necessary and sufficient for enhanced immunity against RSV infection

To assess if the *H. polygyrus*-induced increase in lung mononuclear phagocytes contributes to the previously reported *H. polygyrus* induced antiviral effect against RSV, monocytes were depleted through administration of anti-CCR2 (MC-21) antibodies seven and 9 days after *H. polygyrus* infection. Flow cytometry analysis of tail vein blood 10 dpi confirmed that the antibody treatment reversed the expansion of circulatory monocytes, returning their numbers to steady state levels (Figure 6A). Subtyping of circulatory monocytes confirmed this effect was upon $Ly6C^+Treml4^-$ classical monocytes (Figure S6). Anti-CCR2 treatment also prevented the increases in mononuclear phagocytes (Figure 6B), $Ly6C^+$mononuclear phagocytes (Figure 6C) and $CD11c^+$ mononuclear phagocytes (Figure 6D) in the lung. No other cell population known to be important for control of viral burden was depleted by the anti-CCR2 treatment (Figure S7). Mice were then intranasally infected with 10^5 pfu RSV and their lungs were assessed for viral load by immunoplaque assay 4 days post RSV infection (14 days after *H. polygyrus* infection). The RSV load was significantly reduced following *H. polygyrus* infection, as expected. However, prior anti-CCR2 treatment prevented this decrease in RSV load (Figure 6E). This demonstrates that increases in circulatory monocytes and lung mononuclear phagocytes are required for the *H. polygyrus* induced protective effect against RSV infection.

To complement these depletion experiments, we used adoptive monocyte transfer to test if elevated numbers of blood monocytes are sufficient to replicate the *H. polygyrus* effect and limit RSV infection. Female BALB/c mice were infected with *H. polygyrus* and 10 days later bone marrow was isolated and enriched for monocytes to 94% using negative lineage selection beads to minimise monocyte activation. Two million monocytes from *H. polygyrus* infected or control mice were intravenously transferred to naïve mice to raise their number in the circulation immediately prior to RSV infection. Analysis of the peak

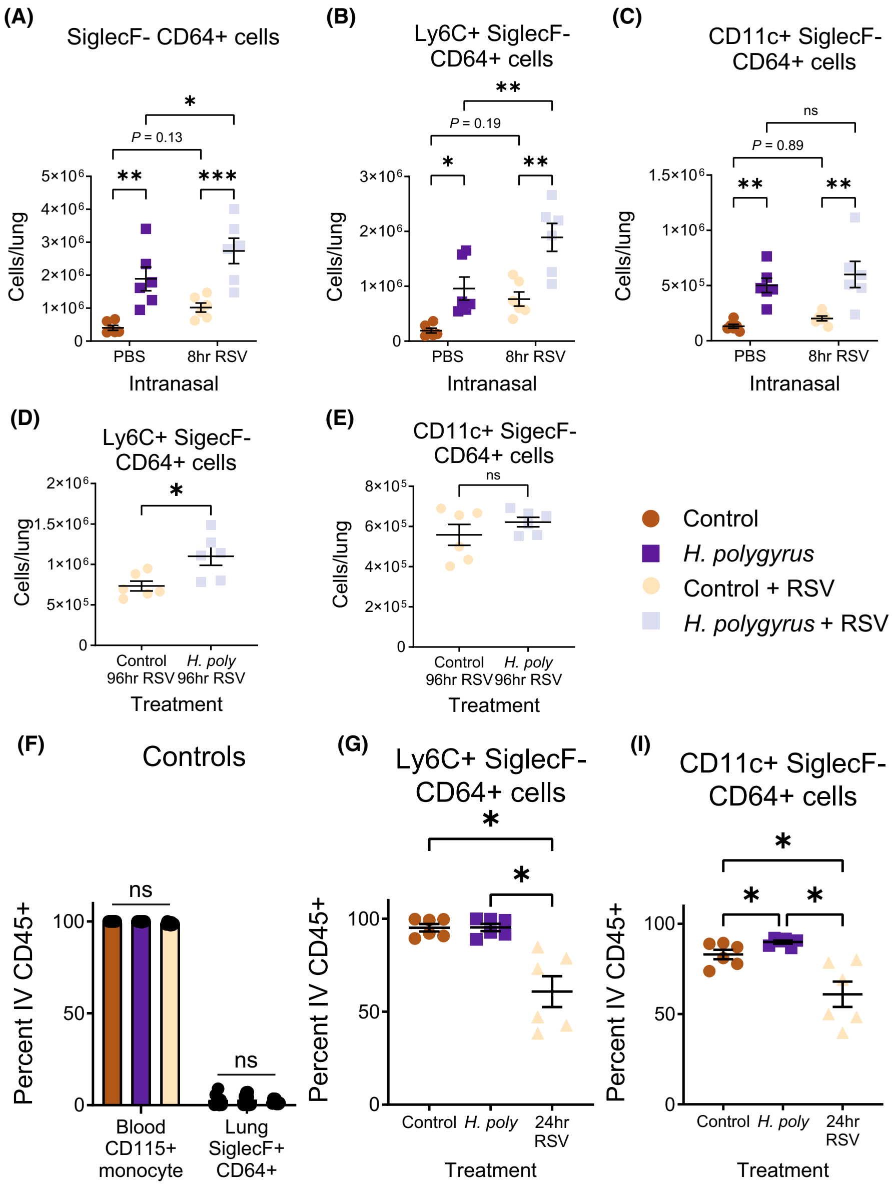

FIGURE 5 *H. polygyrus* infection accelerates accumulation of mononuclear phagocytes in early RSV infection. (A-E) Female BALB/c mice were administered 200 *H. polygyrus* (*H. poly*) L3 larvae by oral gavage or an equal volume of sterile dH_2O as infection control and 10 days post infection (dpi) intranasally administered 10^5 pfu RSV or sterile PBS as infection control then culled 8 h later and numbers of (A) lung mononuclear phagocytes (MNPs), (B) $Ly6C^+$ MNPs and (C) $CD11c^+$ MNPs were assessed by flow cytometry. (D) 96 h post RSV administration with and without prior *H. polygyrus* infection MNP $Ly6C^+$ and (E) $CD11c^+$ subsets were also assessed. (F-I) Female BALB/c mice were administered 200 *H. polygyrus* L3 larvae by oral gavage or an equal volume of sterile dH_2O as infection control then culled 10 dpi. Separately female BALB/c mice were intranasally administered 10^5 pfu RSV and culled 24 h later. Immediately prior to cull all mice were intravenously (IV) administered PE/Cy7 labelled anti CD45. Percentages of (F) blood monocytes and lung SiglecF+ CD64+ alveolar macrophages, (G) Lung Ly6C+ MNPs and (H) CD11c+MNPs labelled with IV CD45 were calculated. Symbols represent individual mice with $n = 6$ per group pooled from two independent experiments. Statistical significance of difference determined with one way ANOVA or with unpaired two-tailed *t*-test. *$p < .05$, **$p < .01$, ***$p < .001$, ns, not significant.

viral load 4 days after RSV infection showed significant decreases in RSV titres after adoptive monocyte transfer from both control and *H. polygyrus* infected animals. Taken together, these data demonstrate that increasing the numbers of circulatory monocytes is sufficient to increase anti-RSV immunity irrespective of the infection state of the donors (Figure 6F). Transfers were repeated on the C57BL/6 background with and without *Ifnar1* expression to test the importance of IFN-I signalling for the antiviral effects of mononuclear phagocytes. All monocytes reduced peak viral load as assessed by RSV L gene expression (Figure 6G). Bulk intravenous administration is known to lead to accumulation of the donor population in the lungs,[36] suggesting that Infar signalling is only required for elevated numbers in the circulation and lung during *H. polygyrus* infection, but is dispensable for their subsequent antiviral properties upon reaching the lung.

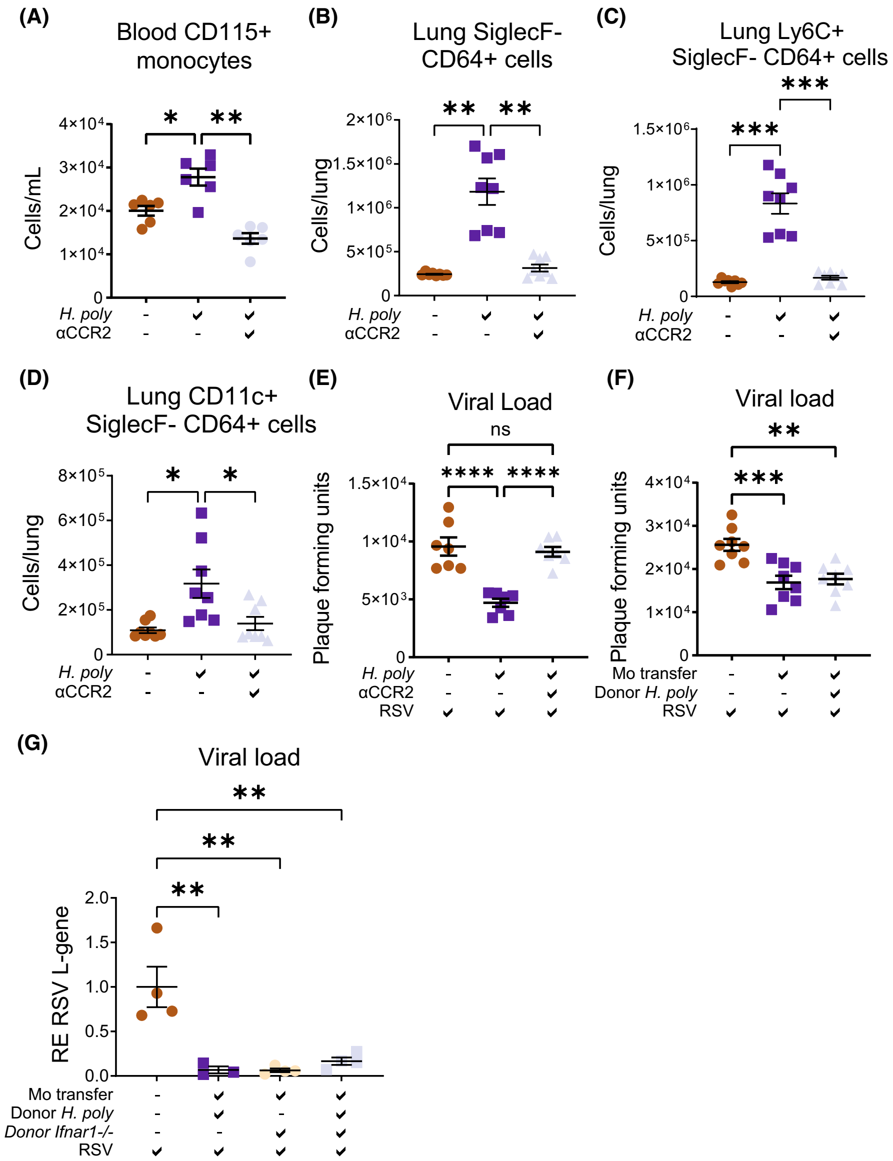

FIGURE 6 Circulatory monocytes are necessary and sufficient for the anti-RSV effects of *H. polygyrus* infection. Female BALB/c mice were administered *H. polygyrus* (*H. poly*) L3 larvae or dH_2O as an infection control by oral gavage. At 7 and 9 days post infection (dpi) the *H. polygyrus* infected animals were administered anti-CCR2 antibody (MC-21) or IgG2b isotype control antibody by intraperitoneal injection. (A) Blood CD115$^+$ monocyte counts at 10 dpi. A subset of mice were culled at 10 dpi to assess numbers of (B) mononuclear phagocytes (MNPs), (C) Ly6C$^+$ MNPs and (D) CD11c$^+$ MNPs in the lung. All remaining mice were infected intranasally with 10^5 pfu RSV. (E) Four days post RSV infection viral load was assessed by immunoplaque assays. (F) Bone marrow was collected from female BALB/c mice 10 dpi with *H. polygyrus* or treatment with dH_2O as a control. Samples were enriched for bone marrow monocytes using magnetic bead negative lineage selection and 2 million monocytes per mouse were administered intravenously via the tail vein 30 min prior to RSV inoculation. PBS was used as a control for monocyte administration. Viral load at 4 dpi RSV was assessed by immunoplaque assay. (G) Monocyte transfer was repeated with male and female C57BL/6 recipients and donor monocytes from *H. polygyrus* infected C57BL/6 mice or *Ifnar1−/−* mice 10 dpi with *H. polygyrus* or dH_2O control. Symbols represent individual mice with $n=6$ per group pooled from two independent experiments for blood CD115+ monocytes (A). $n=8$ per group pooled from three independent experiments for lung MNPs (B-D). For dual infection $n=7$ across two independent experiments viral load assessment (E). Eight mice across two experiments for BALB/c monocyte transfer experiment (F). One experiment with $n=4$ per group for C57BL/6 and *Ifnar1−/−* monocyte transfer experiment (G). Statistical significance of difference determined by one-way ANOVA with multiple comparisons. *$p<.05$, **$p<.01$, ***$p<.001$, ****$p<.0001$, ns, not significant.

3.6 | Expanded mononuclear phagocytes exhibit a pro-inflammatory transcriptomic profile

The number of mononuclear phagocytes within or associated with the lung is clearly central to the early control of RSV burden including in *H. polygyrus* driven expansion. Transfer of bone marrow derived monocytes was suggestive that this numerical effect was sufficient for protection. However, these cells are particularly naïve and lack the further differentiation that occurs within the circulatory environment.[37] To test if the transcriptomic profile of mononuclear

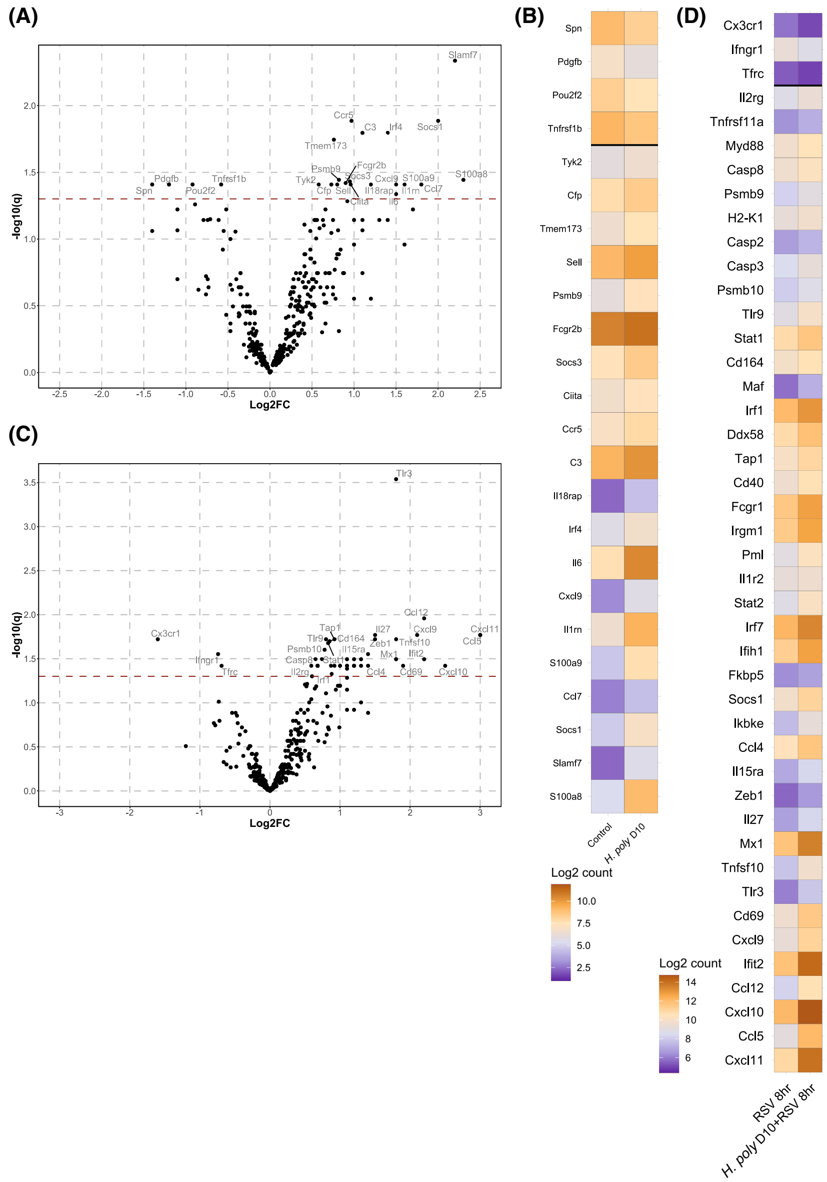

FIGURE 7 *H. polygyrus* induced lung mononuclear phagocytes are transcriptionally distinct in both single and RSV coinfection. Female BALB/c mice were administered an equal volume of either sterile dH_2O as infection control or 200 *H. polygyrus* L3 larvae by oral gavage. Ten days post infection (dpi) lungs were harvested for flow cytometry assisted cell sorting. 8 h prior to cull, some mice of each group were intranasally administered 10^5 pfu RSV. RNA was extracted from isolated Ly6C$^+$ SiglecF$^-$ CD64$^+$ cells and analysed with an nCounter mouse immunology panel. (A) Volcano plot of differentially expressed genes between 10 dpi *H. polygyrus* and infection control. (B) Heatmap of average expression for significantly differentially expressed genes between infection control and 10dpi *H. polygyrus*. (C) Volcano plot of differentially expressed genes between 10dpi *H. polygyrus* post 8 h RSV, and infection control post 8 h RSV. (D) Heatmap of average expression for significantly differentially expressed genes between infection control post 8 h RSV and 10dpi *H. polygyrus* post 8 h RSV. One experimental repeat with $n = 3$ per group. Normalised data for heatmaps were generated using RUVg method from the RUVSeq R package. Differential expression data for volcano plots, plotting −log10(q) against log2-fold change (log2FC), was generated using limma package applied to the RUVg-normalized data. The Benjamini–Hochberg method was used to control for false discovery rate (q). A horizontal red dashed line indicates $q = 0.05$.

phagocytes was altered during *H. polygyrus* infection, targeted transcriptional profiling using the NanoString nCounter platform was performed on flow cytometry sorted lung Ly6C$^+$ SiglecF$^-$ CD64$^+$ cells (Figure 7). A small but significant group of genes associated with inflammatory responses were differentially expressed in *H. polygyrus* primed cells, including *Il6*, *Ccr5* and *Ccl7* (Figure 7A,B). Similarly, we compared gene expression on the same immune panel 8 h post RSV infection with or without prior *H. polygyrus* infection. A different group of genes, associated with anti-viral responses were upregulated by prior *H. polygyrus* infection in this context, including *Mx1* and *Irf7* (Figure 7C,D). Both with and without RSV, *H. polygyrus* also led to the downregulation of genes associated with non-classical monocyte differentiation (*Spn*, *Pou2f2*, *Cx3cr1*). Thus, *H. polygyrus* primed mononuclear phagocytes appear different in nature to their control counterparts.

4 | DISCUSSION

H. polygyrus infection reduces RSV infection peak viral load, secondary immuno-pathology and associated lung function impairment.[6] We now describe how this helminth infection induces enhanced monopoiesis in the bone marrow, elevated circulatory monocytes and increased recruitment of monocyte derived mononuclear phagocytes to the lung. Using monocyte ablation and transfer we show the functional importance of circulatory monocyte derived cells in the *H. polygyrus*-induced anti-viral effect against RSV. Immune gene expression profiling suggests inflammatory changes in these cells that could contribute to antiviral control. Elevated numbers of circulatory leukocytes over the first 2 weeks of *H. polygyrus* infection, including lymphocytes, neutrophils and monocytes have previously been described but only in C57BL/6 mice.[38,39] The correlative observations of bone marrow myelopoiesis to drive this expansion in circulatory monocytes, the subsequent elevation of lung mononuclear phagocytes, and their transcriptional changes are novel to our study. We expect that the mononuclear phagocyte population in the lung is directly derived from circulatory monocytes. This is supported by the circulatory increase being observed from 7 dpi, whereas lung mononuclear phagocytes remain unchanged until 10 dpi, as well as their high proportion of vascular labelling. The absence of the increase in lung mononuclear phagocytes when circulatory monocytes are ablated through both anti-CCR2 treatment or in *Ifnar1−/−* background supports this interpretation. However, due to the potential for persistence of CCR2 on tissue mononuclear phagocytes[40] we cannot discount the possibility that we directly ablated cells in the lung as well.

A growing body of work has assessed the interplay between parasitic and viral infections.[41] *H. polygyrus* infection has been previously described to suppress influenza A (IAV) infection although the mechanism was undetermined.[42] *Trichinella spiralis* infection improves disease outcome to IAV in a gut damage dependent mechanism, but this was through suppression of secondary inflammation, rather than reduction in viral titres and no alteration in the mononuclear phagocyte compartment was observed.[43] *Schistosoma mansoni* (*S. mansoni*) infection is protective against secondary infection with IAV and in pneumonia virus of mice (PVM) infection it gave a small reduction in peak PVM load.[44] *S. mansoni* larvae pass through the lung in mice so their effect on respiratory viral infection is likely due to local inflammatory responses rather than to the systemic response observed with the strictly enteric *H. polygyrus*. A mononuclear phagocyte response was not reported but others have described *S. mansoni* to drive recruitment of alternatively activated macrophages.[45] Their local immunosuppressive effect is often detrimental to viral infection control, with both *H. polygyrus* and *S. mansoni* infection reactivating latent murine γ-herpesvirus infections by suppressing the antiviral IFN response.[46]

Potential links between monocytosis and helminth infections have also been reported in human observational studies. The hookworm *Necator americanus* may increase blood monocyte numbers, and in combination with tuberculosis specifically promoted non-classical monocytes.[47,48] Non-classical monocyte expansion was also observed with the roundworm *Ascaris lumbricoides* both with and without a tuberculosis infection. Helminth infections may also prime human monocytes to produce inflammatory cytokines upon secondary ex vivo LPS stimulation.[49] However, it is important to note that both these parasites have multi-tissue lifecycles, damaging both the gut and the lung mucosa, potentially leading to a more sustained monocytosis than we report with *H. polygyrus*. This is particularly important in observational studies where the time of initial infection is unknown.

The promotion of alternatively activated macrophages in helminth infection has also been described in tissues peripheral to the gut. *H. polygyrus* induces heart macrophages with a strong type 2 polarisation which appear at 28 dpi.[50] The absence of elevated blood monocytes at the late time points in this and our studies further indicates that separate mechanisms are responsible for the early induction of lung mononuclear phagocytes, and a later type-2 immunity driven expansion of alternatively activated macrophages after *H. polygyrus* infection. The lack of upregulation of the M2 marker CD301 10 dpi with irradiated *H. polygyrus* larvae, an infection that still confers monocytosis and is protective against RSV, supports this interpretation (Figure S3C–D). Irradiated larvae still burrow into the duodenal mucosa, suggesting that this initial damage and/or the associated microbiota translocation may be key for inducing monocytosis.

An active factor driving the early *H. polygyrus* effects observed in our study has not yet been identified but the fact that the anti-viral effect and the expansion of both blood monocytes and lung mononuclear phagocytes depend on Infar signalling likely implies a role for IFN-Is either as direct effectors or stimuli for a secondary signal. IFN-I signalling is key to myeloid responses in many other infections. Infar-deficient mice have been used widely in SARS-CoV-2 models where this disruption impairs recruitment of Ly6C$^+$ monocytes to the lung.[51,52] In other inflammatory conditions this may be due to decreased turnover to Ly6C$^-$ monocytes, but the overall increase in total monocyte and mononuclear phagocyte numbers in *H. polygyrus* infection suggests other additional effects.[14] Infar signalling has also been linked to mononuclear phagocyte function in IAV infection[53,54] and to inflammatory monocyte accumulation in mucosal herpes simplex virus infection.[55] IFN-I signalling is also key to the accumulation of inflammatory Ly6C$^+$ mononuclear phagocytes in the lung associated with older age, with a phenotype similar to that seen in viral infections such as IAV.[56] In PVM infection Infar signalling has no effect on monocytic cells but is required for the induction of inflammatory conventional dendritic cells, indicating a likely infection specificity of myeloid IFN-I signalling requirements.[57] However, dendritic cells express CD11c and may contribute to the CD11c$^+$ macrophages we have found to expand after *H. polygyrus* infection. Indeed, the ongoing difficulty in characterising the mononuclear phagocyte sub-compartments in murine pulmonary inflammation (recently reviewed[58,59]) due to shared expression of the key markers used for steady state characterisation is also a limitation in this study. It is important to note that similar to the work in our study, the use of global Infar knockouts in the studies above means that despite the usually high expression of Infar on monocytes, their response may be dependent on secondary cells, supported by the anti-viral activity of administering *Ifnar1–/–* monocytes to an Infar-competent animal.

Effects of IFN-Is on blood monocytes are less well studied including in *Ifnar1* deficiency. The historical characterisations of Infar-deficient mice showed elevated circulatory monocytes, counter to our model, but the increased risk of infection in Infar-deficient mice, at a time before modern infection control measures in animal husbandry were available, may have contributed to this effect.[20] Roles for Ifnar in regulation of bone marrow egress and induction of haematopoiesis may also be factors.[17,60] In human peripheral blood mononuclear cells (PBMCs), classical monocytes are more responsive to IFN-Is than non-classical monocytes due to differential abundance of Infar[61] and culture of PBMCs with IFN-Is will alter their phenotype.[62–64] An expansion of circulatory monocytes and lung $CD64^+$ cells, similar to our findings, was observed in idiopathic pulmonary fibrosis patients and associated with increased circulatory IFN-Is.[65] Exogenous treatment with IFNα for 2–4 weeks in asthma patients also increased the numbers of circulating monocytes and increased their antigen presenting phenotype.[66]

Clearly, from the array of responses described above the context of IFN-I signalling is crucial. The outcome of IFN-I stimulation is modulated by concomitant signalling/environmental factors that certainly also play a role in *H. polygyrus* responses.[67] One such environmental factor is the microbiome and its metabolic products, the presence of which is essential for the *H. polygyrus* antiviral effect.[6] While we were unable to test the impact of the microbiome in the present study, interactions between IFN-I production and microbiome components have been well described[68,69] and the microbiome is known to be modulated in helminth infections including *H. polygyrus* infection.[70,71]

The apparent lack of dependency on Infar signalling for bone marrow monopoiesis in this model suggests alternative signalling requirements. Interferon treatments have been described to affect lymphopoiesis,[72] IFN-I suppresses neutrophil differentiation,[73,74] and IFNγ promotes myelopoiesis.[75,76] Parasitic modulation of the bone marrow has also been described, with *Trichuris muris* and *Toxoplasma gondii* infections modulating haematopoiesis in an IFNγ dependent manner.[15,77] There is also substantial evidence that interferon regulatory factor 5 (IRF5) is a key regulator of hematopoietic development, particularly in myeloid lineages.[78,79] *H. polygyrus* has been recently described to induce IFN-γ (IFN-II) early in infection[80] which may be responsible for the initial induction of monopoiesis. The deeply interlinked feedback loops between IFN-I and IFN-II signalling may explain why we see a reduced effect on monocytosis in the bone marrow.[81]

The exact mechanism of the anti-viral effect of *H. polygyrus*-induced mononuclear phagocytes is still unclear. Mononuclear phagocytes in RSV infection are known to produce TNFα, which is important for the control of viral expansion, providing a possible mechanism,[13] but their direct effects on viral load were not assessed. Our findings directly demonstrate, for the first time, that elevating mononuclear phagocyte numbers in the lung prior to RSV infection can reduce viral load. Monocytes/macrophages are also known to produce IFNβ, viperin and OAS in response to viral exposure, thus the expansion of mononuclear phagocytes in the lung may explain the previously observed increase in these antiviral factors in whole lung samples during *H. polygyrus* infection.[19,82–84] Our transcriptional analysis of the $Ly6C^+$ mononuclear phagocyte compartment suggests that *H. polygyrus* induced cells may be primed for infection response. Inflammatory proteins S100a8, S100a9 and C3 have been associated with lung damage in severe viral infection but their upregulation in early infection may be beneficial to viral control.[85,86] Complement products including C3 have also been observed to coat RSV-infected epithelial cells in historical studies.[87–89] Many interferon signalling and interferon regulatory pathways are further enhanced in early RSV infection by the prior *H. polygyrus* infection. Myd88 signalling is essential for the induction of Ifnβ expression in monocytes[19] while TLR and Stat pathways are central to many interferon-stimulated gene networks.[90] Mx1 is a known viral restriction factor. Interrogation of highlighted interferon associated signalling pathways will be of particular interest for future investigations.[91] Many other cytokines and chemokines that were found to be induced across these datasets may promote antiviral immunity. IL-6 is induced in both human and murine RSV infection, and is thought to be critical for regulating the immune response during RSV infection.[92,93] Indeed elevated IL-6 was previously observed in our whole lung analysis of *H. polygyrus* infection,[6] Ccl5, 7, and 12 and Cxcl9, 10 and 11 likely promote the recruitment of a wide array of innate and adaptive immune cells that can contribute to the RSV immune response.

The transcriptomic analysis also aligns with our characterisation of monocytic dynamics. Amongst the downregulated genes are many that are associated with non-classical monocytes, specifically *Spn* (Cd43), *Pou2f2* and *Cx3cr1*, supporting the generation of new $Ly6C^+$ classical monocytes from the bone marrow suggesting that these are the source of $Ly6C^+$ mononuclear phagocytes. The upregulation of *Sell* (L-selectin) may also provide a mechanism through which the initial wave of circulatory monocytes leads to the secondary accumulation of monocytes/mononuclear phagocytes within the lung whilst still being freely available to intravenous labelling. L-selectin is a key receptor in the process of endothelial tethering and rolling required for latter extravasation.[37,94] CCR5 and CD69 upregulation may also be indicative of monocytic cells associating with the tissue and maturing.[95]

In conclusion, we show that intestinal helminth infection can induce transient systemic monocytosis and increased numbers of mononuclear phagocytes within the lung that are essential to reducing the burden of viral respiratory infection. Due to the Infar dependency of this expansion in the blood and lung we hypothesise that helminth induced IFN-Is or secondary signalling products play a key role in these effects. Future work will be required to identify the specific factors that act upon monocytes to drives these effects and to further characterise the specific anti-viral mechanisms of these cells in RSV infection.

AUTHOR CONTRIBUTIONS

Study design by MOB, SJJ, CBB, HJMcS and JS. Experiments performed by MOB with PJ, KB for flow cytometry and with HM for Methocult assays. PJ performed data processing for nCounter. MOB, CCB and HJMcS analysed and discussed the data with JS. MOB and JS drafted the manuscript and MOB, HM, SJJ, CCB, HJMcS and JS critically reviewed and revised the manuscript. JS obtained the funding. MM developed and provided the MC-21 antibody. All authors gave final approval to the version submitted for publication.

ACKNOWLEDGMENTS

Flow cytometry data were generated with support from the QMRI Flow Cytometry and cell sorting facility, University of Edinburgh. We acknowledge Alison Munro of HTPU Microarray Services at the Institute of Genetics and Cancer for their technical support. This work was funded by UKRI-MRC grant MR/T029668/1. This UK funded award is part of the EDCTP2 programme supported by the European Union. CCB is supported by a Sir Henry Dale Fellowship jointly funded by the Wellcome Trust and the Royal Society (grant number 206234/Z/17/Z). For the purpose of open access, the author has applied a Creative Commons Attribution (CC BY) licence to any Author Accepted Manuscript version arising from this submission. We thank Amy Buck (University of Edinburgh, United Kingdom) for providing *H. polygyrus* L3 larvae and Samanta Mariani (University of Edinburgh, United Kingdom) for advice on bone marrow Methocult assays.

CONFLICT OF INTEREST STATEMENT

The authors declare no conflict of interest in relation to this work.

DATA AVAILABILITY STATEMENT

The data that support the findings of this study are available from the corresponding author upon reasonable request.

ORCID

Matthew O. Burgess https://orcid.org/0000-0001-9666-6787
Stephen J. Jenkins https://orcid.org/0000-0002-0233-5424
Jurgen Schwarze https://orcid.org/0000-0002-6899-748X

REFERENCES

1. GBD 2016 Lower Respiratory Infections Collaborators. Estimates of the global, regional, and national morbidity, mortality, and aetiologies of lower respiratory infections in 195 countries, 1990–2016: a systematic analysis for the global burden of disease study 2016. *Lancet Infect Dis*. 2018;18(11):1191-1210.
2. Falsey AR, Hennessey PA, Formica MA, Cox C, Walsh EE. Respiratory syncytial virus infection in elderly and high-risk adults. *N Engl J Med*. 2005;352(17):1749-1759.
3. Nguyen-Van-Tam JS, O'Leary M, Martin ET, et al. Burden of respiratory syncytial virus infection in older and high-risk adults: a systematic review and meta-analysis of the evidence from developed countries. *Eur Respir Rev*. 2022;31(166):220105.
4. Binns E, Tuckerman J, Licciardi PV, Wurzel D. Respiratory syncytial virus, recurrent wheeze and asthma: a narrative review of pathophysiology, prevention and future directions. *J Paediatr Child Health*. 2022;58(10):1741-1746.
5. Soto JA, Stephens LM, Waldstein KA, Canedo-Marroquin G, Varga SM, Kalergis AM. Current insights in the development of efficacious vaccines against RSV. *Front Immunol*. 2020;11:1507.
6. McFarlane AJ, McSorley HJ, Davidson DJ, et al. Enteric helminth-induced type I interferon signaling protects against pulmonary virus infection through interaction with the microbiota. *J Allergy Clin Immunol*. 2017;140:1068-1078.
7. Maizels RM. Regulation of immunity and allergy by helminth parasites. *Allergy*. 2020;75(3):524-534.
8. Schoggins JW. Interferon-stimulated genes: what Do they all Do? *Annu Rev Virol*. 2019;6(1):567-584.
9. Schoggins JW, Wilson SJ, Panis M, et al. A diverse range of gene products are effectors of the type I interferon antiviral response. *Nature*. 2011;472(7344):481-485.
10. Khaitov MR, Laza-Stanca V, Edwards MR, et al. Respiratory virus induction of alpha-, beta- and lambda-interferons in bronchial epithelial cells and peripheral blood mononuclear cells. *Allergy*. 2009;64(3):375-386.
11. Sposito B, Broggi A, Pandolfi L, et al. The interferon landscape along the respiratory tract impacts the severity of COVID-19. *Cell*. 2021;184(19):4953-4968.
12. McNab F, Mayer-Barber K, Sher A, Wack A, O'Garra A. Type I interferons in infectious disease. *Nat Rev Immunol*. 2015;15(2):87-103.
13. Goritzka M, Makris S, Kausar F, et al. Alveolar macrophage-derived type I interferons orchestrate innate immunity to RSV through recruitment of antiviral monocytes. *J Exp Med*. 2015;212(5):699-714.
14. Lee PY, Li Y, Kumagai Y, et al. Type I interferon modulates monocyte recruitment and maturation in chronic inflammation. *Am J Pathol*. 2009;175(5):2023-2033.
15. Askenase MH, Han SJ, Byrd AL, et al. Bone-marrow-resident NK cells prime monocytes for regulatory function during infection. *Immunity*. 2015;42(6):1130-1142.
16. Dalmas E, Toubal A, Alzaid F, et al. Irf5 deficiency in macrophages promotes beneficial adipose tissue expansion and insulin sensitivity during obesity. *Nat Med*. 2015;21(6):610-618.
17. Essers MA, Offner S, Blanco-Bose WE, et al. IFNalpha activates dormant haematopoietic stem cells in vivo. *Nature*. 2009;458(7240):904-908.
18. Krausgruber T, Blazek K, Smallie T, et al. IRF5 promotes inflammatory macrophage polarization and TH1-TH17 responses. *Nat Immunol*. 2011;12(3):231-238.
19. Kim TH, Kim CW, Oh DS, Jung HE, Lee HK. Monocytes contribute to IFN-beta production via the MyD88-dependent pathway and cytotoxic T-cell responses against mucosal respiratory syncytial virus infection. *Immune Netw*. 2021;21(4):e27.
20. Muller U, Steinhoff U, Reis LF, et al. Functional role of type I and type II interferons in antiviral defense. *Science*. 1994;264(5167):1918-1921.
21. Johnston CJ, Robertson E, Harcus Y, et al. Cultivation of Heligmosomoides polygyrus: an immunomodulatory nematode parasite and its secreted products. *J Vis Exp*. 2015;98:e52412.
22. Currie SM, Findlay EG, McHugh BJ, et al. The human cathelicidin LL-37 has antiviral activity against respiratory syncytial virus. *PLoS One*. 2013;8(8):e73659.
23. Class CA, Lukan CJ, Bristow CA, Do KA. Easy NanoString nCounter data analysis with the NanoTube. *Bioinformatics*. 2023;39(1):btac762.

24. Risso D, Ngai J, Speed TP, Dudoit S. Normalization of RNA-seq data using factor analysis of control genes or samples. *Nat Biotechnol*. 2014;32(9):896-902.
25. Ritchie ME, Phipson B, Wu D, et al. Limma powers differential expression analyses for RNA-sequencing and microarray studies. *Nucleic Acids Res*. 2015;43(7):e47.
26. Hawley CA, Rojo R, Raper A, et al. Csf1r-mApple transgene expression and ligand binding in vivo reveal dynamics of CSF1R expression within the mononuclear phagocyte system. *J Immunol*. 2018;200(6):2209-2223.
27. Plantinga M, Guilliams M, Vanheerswynghels M, et al. Conventional and monocyte-derived CD11b(+) dendritic cells initiate and maintain T helper 2 cell-mediated immunity to house dust mite allergen. *Immunity*. 2013;38(2):322-335.
28. Ingersoll MA, Spanbroek R, Lottaz C, et al. Comparison of gene expression profiles between human and mouse monocyte subsets. *Blood*. 2010;115(3):e10-e19.
29. Tacke F, Randolph GJ. Migratory fate and differentiation of blood monocyte subsets. *Immunobiology*. 2006;211(6–8):609-618.
30. Shalash AO, Hussein WM, Skwarczynski M, Toth I. Hookworm infection: toward development of safe and effective peptide vaccines. *J Allergy Clin Immunol*. 2021;148(6):1394-1419.
31. Behnke JM. Structure in parasite component communities in wild rodents: predictability, stability, associations and interactions … Or pure randomness? *Parasitology*. 2008;135(7):751-766.
32. Pleass RJ, Bianco AE. The effects of gamma radiation on the development of Heligmosomoides polygyrus bakeri in mice. *Int J Parasitol*. 1995;25(9):1099-1109.
33. Hettinger J, Richards DM, Hansson J, et al. Origin of monocytes and macrophages in a committed progenitor. *Nat Immunol*. 2013;14(8):821-830.
34. Yona S, Kim KW, Wolf Y, et al. Fate mapping reveals origins and dynamics of monocytes and tissue macrophages under homeostasis. *Immunity*. 2013;38(1):79-91.
35. Thomas GD, Hanna RN, Vasudevan NT, et al. Deleting an Nr4a1 super-enhancer subdomain ablates Ly6C(low) monocytes while preserving macrophage gene function. *Immunity*. 2016;45(5):975-987.
36. Fischer UM, Harting MT, Jimenez F, et al. Pulmonary passage is a major obstacle for intravenous stem cell delivery: the pulmonary first-pass effect. *Stem Cells Dev*. 2009;18(5):683-692.
37. Jakubzick CV, Randolph GJ, Henson PM. Monocyte differentiation and antigen-presenting functions. *Nat Rev Immunol*. 2017;17(6):349-362.
38. Ali NM, Behnke JM, Manger BR. The pattern of peripheral blood leucocyte changes in mice infected with Nematospiroides dubius. *J Helminthol*. 1985;59(1):83-93.
39. Baker NF. The nature and etiology of the leukocytic response of Webster mice infected with Nematospiroides dubius. *J Parasitol*. 1962;48:438-441.
40. Dick SA, Wong A, Hamidzada H, et al. Three tissue resident macrophage subsets coexist across organs with conserved origins and life cycles. *Sci Immunol*. 2022;7(67):eabf7777.
41. Desai P, Diamond MS, Thackray LB. Helminth-virus interactions: determinants of coinfection outcomes. *Gut Microbes*. 2021;13(1):1961202.
42. Chowaniec W, Wescott RB, Congdon LL. Interaction of Nematospiroides dubius and influenza virus in mice. *Exp Parasitol*. 1972;32(1):33-44.
43. Furze RC, Hussell T, Selkirk ME. Amelioration of influenza-induced pathology in mice by coinfection with trichinella spiralis. *Infect Immun*. 2006;74(3):1924-1932.
44. Scheer S, Krempl C, Kallfass C, et al. S. Mansoni bolsters anti-viral immunity in the murine respiratory tract. *PLoS One*. 2014;9(11):e112469.
45. Santos MP, Goncalves-Santos E, Goncalves RV, et al. Doxycycline aggravates granulomatous inflammation and lung microstructural remodeling induced by Schistosoma mansoni infection. *Int Immunopharmacol*. 2021;94:107462.
46. Reese TA, Wakeman BS, Choi HS, et al. Helminth infection reactivates latent gamma-herpesvirus via cytokine competition at a viral promoter. *Science*. 2014;345(6196):573-577.
47. Passos LS, Gazzinelli-Guimaraes PH, Oliveira Mendes TA, et al. Regulatory monocytes in helminth infections: insights from the modulation during human hookworm infection. *BMC Infect Dis*. 2017;17(1):253.
48. Bewket G, Kiflie A, Abate E, Stendahl O, Schon T, Blomgran R. Helminth species specific expansion and increased TNF-alpha production of non-classical monocytes during active tuberculosis. *PLoS Negl Trop Dis*. 2021;15(3):e0009194.
49. Jackson JA, Turner JD, Kamal M, et al. Gastrointestinal nematode infection is associated with variation in innate immune responsiveness. *Microbes Infect*. 2006;8(2):487-492.
50. Mylonas KJ, Jenkins SJ, Castellan RF, et al. The adult murine heart has a sparse, phagocytically active macrophage population that expands through monocyte recruitment and adopts an 'M2' phenotype in response to Th2 immunologic challenge. *Immunobiology*. 2015;220(7):924-933.
51. Channappanavar R, Fehr AR, Vijay R, et al. Dysregulated type I interferon and inflammatory monocyte-macrophage responses cause lethal pneumonia in SARS-CoV-infected mice. *Cell Host Microbe*. 2016;19(2):181-193.
52. Ogger PP, Garcia Martin M, Michalaki C, et al. Type I interferon receptor signalling deficiency results in dysregulated innate immune responses to SARS-CoV-2 in mice. *Eur J Immunol*. 2022;52(11):1768-1775.
53. Garcia-Sastre A, Durbin RK, Zheng H, et al. The role of interferon in influenza virus tissue tropism. *J Virol*. 1998;72(11):8550-8558.
54. Price GE, Gaszewska-Mastarlarz A, Moskophidis D. The role of alpha/beta and gamma interferons in development of immunity to influenza a virus in mice. *J Virol*. 2000;74(9):3996-4003.
55. Lee AJ, Chen B, Chew MV, et al. Inflammatory monocytes require type I interferon receptor signaling to activate NK cells via IL-18 during a mucosal viral infection. *J Exp Med*. 2017;214(4):1153-1167.
56. D'Souza SS, Zhang Y, Bailey JT, et al. Type I interferon signaling controls the accumulation and transcriptomes of monocytes in the aged lung. *Aging Cell*. 2021;20(10):e13470.
57. Bosteels C, Neyt K, Vanheerswynghels M, et al. Inflammatory type 2 cDCs acquire features of cDC1s and macrophages to orchestrate immunity to respiratory virus infection. *Immunity*. 2020;52(6):1039-1056.
58. Aegerter H, Lambrecht BN, Jakubzick CV. Biology of lung macrophages in health and disease. *Immunity*. 2022;55(9):1564-1580.
59. T'Jonck W, Bain CC. The role of monocyte-derived macrophages in the lung: It's all about context. *Int J Biochem Cell Biol*. 2023;159:106421.
60. Jia T, Leiner I, Dorothee G, Brandl K, Pamer EG. MyD88 and type I interferon receptor-mediated chemokine induction and monocyte recruitment during listeria monocytogenes infection. *J Immunol*. 2009;183(2):1271-1278.
61. Han S, Zhuang H, Lee PY, et al. Differential responsiveness of monocyte and macrophage subsets to interferon. *Arthritis Rheumatol*. 2020;72(1):100-113.
62. Dickensheets HL, Donnelly RP. Inhibition of IL-4-inducible gene expression in human monocytes by type I and type II interferons. *J Leukoc Biol*. 1999;65(3):307-312.
63. Pogue SL, Preston BT, Stalder J, Bebbington CR, Cardarelli PM. The receptor for type I IFNs is highly expressed on peripheral blood B cells and monocytes and mediates a distinct profile of

differentiation and activation of these cells. *J Interf Cytokine Res*. 2004;24(2):131-139.
64. Tong Y, Zhou L, Yang L, et al. Concomitant type I IFN and M-CSF signaling reprograms monocyte differentiation and drives pro-tumoral arginase production. *EBioMedicine*. 2019;39:132-144.
65. Fraser E, Denney L, Antanaviciute A, et al. Multi-modal characterization of monocytes in idiopathic pulmonary fibrosis reveals a primed type I interferon immune phenotype. *Front Immunol*. 2021;12:623430.
66. Simon HU, Seelbach H, Ehmann R, Schmitz M. Clinical and immunological effects of low-dose IFN-alpha treatment in patients with corticosteroid-resistant asthma. *Allergy*. 2003;58(12):1250-1255.
67. van Boxel-Dezaire AH, Rani MR, Stark GR. Complex modulation of cell type-specific signaling in response to type I interferons. *Immunity*. 2006;25(3):361-372.
68. Erttmann SF, Swacha P, Aung KM, et al. The gut microbiota prime systemic antiviral immunity via the cGAS-STING-IFN-I axis. *Immunity*. 2022;55(5):847-861.
69. Winkler ES, Shrihari S, Hykes BL Jr, et al. The intestinal microbiome restricts alphavirus infection and dissemination through a bile acid-type I IFN signaling Axis. *Cell*. 2020;182(4):901-918.
70. Kennedy MHE, Brosschot TP, Lawrence KM, et al. Small intestinal levels of the branched short-chain fatty acid isovalerate are elevated during infection with Heligmosomoides polygyrus and can promote helminth fecundity. *Infect Immun*. 2021;89(12):e0022521.
71. Reynolds LA, Smith KA, Filbey KJ, et al. Commensal-pathogen interactions in the intestinal tract: lactobacilli promote infection with, and are promoted by, helminth parasites. *Gut Microbes*. 2014;5(4):522-532.
72. Di Scala M, Gil-Farina I, Vanrell L, et al. Chronic exposure to IFNalpha drives medullar lymphopoiesis towards T-cell differentiation in mice. *Haematologica*. 2015;100(8):1014-1022.
73. Nguyen-Jackson H, Panopoulos AD, Zhang H, Li HS, Watowich SS. STAT3 controls the neutrophil migratory response to CXCR2 ligands by direct activation of G-CSF-induced CXCR2 expression and via modulation of CXCR2 signal transduction. *Blood*. 2010;115(16):3354-3363.
74. Siakaeva E, Pylaeva E, Spyra I, et al. Neutrophil maturation and survival is controlled by IFN-dependent regulation of NAMPT signaling. *Int J Mol Sci*. 2019;20(22):5584.
75. Buechler MB, Akilesh HM, Hamerman JA. Cutting edge: direct sensing of TLR7 ligands and type I IFN by the common myeloid progenitor promotes mTOR/PI3K-dependent emergency myelopoiesis. *J Immunol*. 2016;197(7):2577-2582.
76. Grainger JR, Wohlfert EA, Fuss IJ, et al. Inflammatory monocytes regulate pathologic responses to commensals during acute gastrointestinal infection. *Nat Med*. 2013;19(6):713-721.
77. Chenery AL, Antignano F, Hughes MR, Burrows K, McNagny KM, Zaph C. Chronic Trichuris muris infection alters hematopoiesis and causes IFN-gamma-expressing T-cell accumulation in the mouse bone marrow. *Eur J Immunol*. 2016;46(11):2587-2596.
78. Corbin AL, Gomez-Vazquez M, Berthold DL, et al. IRF5 guides monocytes toward an inflammatory CD11c(+) macrophage phenotype and promotes intestinal inflammation. *Sci Immunol*. 2020;5(47):eaax6085.
79. Schoenemeyer A, Barnes BJ, Mancl ME, et al. The interferon regulatory factor, IRF5, is a central mediator of toll-like receptor 7 signaling. *J Biol Chem*. 2005;280(17):17005-17012.
80. Progatzky F, Shapiro M, Chng SH, et al. Regulation of intestinal immunity and tissue repair by enteric glia. *Nature*. 2021;599(7883):125-130.
81. Michalska A, Blaszczyk K, Wesoly J, Bluyssen HAR. A positive feedback amplifier circuit that regulates interferon (IFN)-stimulated gene expression and controls type I and type II IFN responses. *Front Immunol*. 2018;9:1135.
82. Fagone P, Nunnari G, Lazzara F, et al. Induction of OAS gene family in HIV monocyte infected patients with high and low viral load. *Antivir Res*. 2016;131:66-73.
83. Lee D, Le Pen J, Yatim A, et al. Inborn errors of OAS-RNase L in SARS-CoV-2-related multisystem inflammatory syndrome in children. *Science*. 2023;379(6632):eabo3627.
84. Teng TS, Foo SS, Simamarta D, et al. Viperin restricts chikungunya virus replication and pathology. *J Clin Invest*. 2012;122(12):4447-4460.
85. Foronjy RF, Ochieng PO, Salathe MA, et al. Protein tyrosine phosphatase 1B negatively regulates S100A9-mediated lung damage during respiratory syncytial virus exacerbations. *Mucosal Immunol*. 2016;9(5):1317-1329.
86. Song Z, Bai J, Liu X, et al. S100A9 regulates porcine reproductive and respiratory syndrome virus replication by interacting with the viral nucleocapsid protein. *Vet Microbiol*. 2019;239:108498.
87. Kaul TN, Faden H, Baker R, Ogra PL. Virus-induced complement activation and neutrophil-mediated cytotoxicity against respiratory syncytial virus (RSV). *Clin Exp Immunol*. 1984;56(3):501-508.
88. Edwards KM, Snyder PN, Wright PF. Complement activation by respiratory syncytial virus-infected cells. *Arch Virol*. 1986;88(1–2):49-56.
89. Kaul TN, Welliver RC, Ogra PL. Appearance of complement components and immunoglobulins on nasopharyngeal epithelial cells following naturally acquired infection with respiratory syncytial virus. *J Med Virol*. 1982;9(2):149-158.
90. Ivashkiv LB, Donlin LT. Regulation of type I interferon responses. *Nat Rev Immunol*. 2014;14(1):36-49.
91. Haller O, Arnheiter H, Pavlovic J, Staeheli P. The discovery of the antiviral resistance gene mx: a story of great ideas, great failures, and some success. *Annu Rev Virol*. 2018;5(1):33-51.
92. Pyle CJ, Uwadiae FI, Swieboda DP, Harker JA. Early IL-6 signalling promotes IL-27 dependent maturation of regulatory T cells in the lungs and resolution of viral immunopathology. *PLoS Pathog*. 2017;13(9):e1006640.
93. Chappin K, Besteman SB, Hennus MP, et al. Airway and blood monocyte transcriptomic profiling reveals an antiviral phenotype in infants with severe respiratory syncytial virus infection. *J Infect Dis*. 2024;229(Supplement_1):S100-S111.
94. Ivetic A, Hoskins Green HL, Hart SJ. L-selectin: a major regulator of leukocyte adhesion, migration and signaling. *Front Immunol*. 2019;10:1068.
95. Baeyens A, Bracero S, Chaluvadi VS, Khodadadi-Jamayran A, Cammer M, Schwab SR. Monocyte-derived S1P in the lymph node regulates immune responses. *Nature*. 2021;592(7853):290-295.

SUPPORTING INFORMATION

Additional supporting information can be found online in the Supporting Information section at the end of this article.

How to cite this article: Burgess MO, Janas P, Berry K, et al. Helminth induced monocytosis conveys protection from respiratory syncytial virus infection in mice. *Allergy*. 2024;79:2157-2172. doi:10.1111/all.16206